THE ASTROPHYSICAL JOURNAL, 393:L55–L58, 1992 July 10

LATE DETONATION MODELS FOR THE TYPE Ia SUPERNOVAE SN 1991T AND SN 1990N

HITOSHI YAMAOKA AND KEN'ICHI NOMOTO
Department of Astronomy, Faculty of Science, University of Tokyo, Tokyo, Japan 113
TOSHIKAZU SHIGEYAMA
Max-Planck-Institut für Astrophysik, D8046 Garching bei München, Germany; and
Department of Astronomy, Faculty of Science, University of Tokyo, Tokyo, Japan 113
AND
FRIEDRICH-KARL THIELEMANN
Harvard-Smithsonian Center for Astrophysics, Cambridge, MA 02138
Received 1992 February 18; accepted 1992 April 15

ABSTRACT

We present hydrodynamical models of exploding white dwarfs to account for the newly observed premaximum features of Type Ia supernovae 1990N and 1991T in a unified manner. In these models, a carbon deflagration, producing a central Fe/Co/Ni core and an intermediate Si/S/Ca layer, is later transformed into a detonation in the outermost layer. Depending on the transition density, the nucleosynthesis in such *late* detonations results in the formation of Fe-dominated surface layers or Si/Fe-rich surface layers, which are qualitatively consistent with the inferred composition of SN 1991T and 1990N, respectively.

Subject headings: nucleosynthesis — supernovae: general — supernovae: individual (SN 1990N) — supernovae: individual (SN 1991T) — white dwarfs

1. INTRODUCTION

Recent observations of Type Ia supernovae (SNs Ia) before maximum brightness, providing new information on the composition of the outermost layers of SNs Ia, challenge the current theoretical models (see, e.g., Nomoto et al. 1992 for a review): (1) The premaximum spectra of SN 1990N (Leibundgut et al. 1991) indicate the presence of Si, Ca, Fe, and Co in the outermost layers with $v_{\rm exp} \sim 20{,}000$ km s^{-1}. (2) SN 1991T has shown quite a unique spectral evolution: the premaximum spectrum is dominated by Fe/Ni lines, while the spectra after maximum light show typical SNs Ia features, characterized first by Si/S/Ca lines, and later becoming Fe-dominated (Filippenko et al. 1992; Ruiz-Lapuente et al. 1992).

The inferred composition structure of SN 1991T is as follows: (1) The outermost layer is composed of Ni and Fe with expansion velocities $v_{\rm exp} \sim 13{,}000$ km s^{-1}. (2) The intermediate layer is rich in Si/Ca with $v_{\rm exp} \sim 10{,}000$ km s^{-1}. (3) The central layer is again dominated by Fe (Filippenko et al. 1992). In other words, the Si/S/Ca-rich layer 2 is sandwiched by the two Fe layers (1 and 3). Such a composition *inversion* with Fe above Si is very different from that inferred from typical SNs Ia. On the other hand, the composition of the inner layers (2 and 3) is very similar to those of typical SNs Ia including SN 1990N (Filippenko et al. 1992; Phillips et al. 1992).

The composition of the inner layers 2 and 3 of the above SNs Ia may be accounted for by the carbon deflagration model W7 (Nomoto, Thielemann, & Yokoi 1984, hereafter NTY). However, the presence of high-velocity heavy elements in these SNs Ia is not consistent with W7, because the highest velocities of newly synthesized elements in W7 are $\sim 15{,}000$ km s^{-1} and the outermost layer is dominated by O and C.

Shigeyama et al. (1992) have listed four possible models for SN 1990N. Among them are the following: (1) mixing adds Si, Ca, and Fe to the outer layers of W7 (Branch et al. 1985; Branch & Venkatakrishna 1986); it may, however, be difficult to cause a composition inversion with Fe/Ni in the outermost layers as in SN 1991T. (2) The delayed detonation models assume that an initially very slow deflagration turns into a detonation relatively deep in the interior (Khoklov 1991b; Woosley & Weaver 1992); such an event produces high-velocity Si/Ca, but it is difficult to synthesize Fe again near the surface. (3) The carbon detonation models for low-mass white dwarfs (Shigeyama et al. 1992) have the same difficulty in explaining SN 1991T. If one of the cases 1–3 is the actual model for SN 1990N, then it is likely that SN 1991T resulted from a somewhat different explosion mechanism, thus belonging to a different subclass of SNs I (e.g., SNe Id; Branch & Tammann 1992).

The remaining possibility (4) given in Shigeyama et al. (1992) is the formation of a detonation in the outermost layers, induced by a fast propagation of a deflagration wave. NTY noted that the carbon deflagration model C8, whose propagation velocity $v_{\rm def}$ is ~ 1.2 times higher than W7, has a precursor shock which is strong enough to induce a detonation in the outer layers (see also Woosley & Weaver 1986). In view of the small difference in $v_{\rm def}$ between W7 and C8, the deflagration in W7 can be regarded as marginal in forming a detonation in the outer layers.

The transition from a deflagration to a detonation can occur when the propagation velocity of the deflagration wave $v_{\rm def}$ is accelerated to the Chapman-Jouguet velocity $v_{\rm CJ}$. The transition is more likely to occur at lower densities, because the ratio $v_{\rm CJ}/v_s$ (v_s denotes the sound velocity) is smaller due to a larger density jump across the burning front (Khokhlov 1991a), while $v_{\rm def}/v_s$ is larger (NTY). Since the convective deflagration front may well be quite turbulent and the acceleration of $v_{\rm def}$ may take place in an indeterministic manner, the condition of the transition from deflagration to detonation has not been well understood (e.g., Williams 1985), and it could occur even for $v_{\rm def} < v_{\rm CJ}$. It is also possible that a relatively small

difference in v_{def} in the deeper layers could cause a large variation in the transition density in the outer layers. Such a difference in v_{def} may stem from differences in ignition conditions, such as the central density (i.e., the age and the accretion rate) of the white dwarf.

Although v_{def} is an unknown parameter extremely difficult to determine, recent authors modeling synthetic spectra for generic SNs Ia (Harkness 1991) and also 1990N and 1991T (Jeffrey et al. 1992) all come to the conclusion that the spectra are consistent with W7-like central cores of SNs Ia. Thus we chose to explore variations along this line.

In the present *Letter* we present several hydrodynamical models for case 4; here the carbon deflagration, producing a central Fe/Co/Ni core and an intermediate Si/S/Ca layer, is later transformed into a detonation in the outermost layers, which we call a *late detonation*. We show that nucleosynthesis in the detonated matter depends sensitively on the density at the transition from deflagration to detonation. We suggest that a variation of nucleosynthesis (e.g., ^{56}Ni/Si ratio) in such later detonations may possibly account for both SN 1990N and SN 1991T in a unified manner, that is, SN 1991T may well be a small variant of SNe Ia. In § 2 the adopted deflagration models are described. Nucleosynthesis outcome is shown in § 3. Comparison with observations of SN 1990N and 1991T are summarized in § 4.

2. MODELS

To construct models of SNs Ia, we start from a C + O white dwarf that accretes matter at a rate of $4 \times 10^{-8}\ M_\odot\ \mathrm{yr}^{-1}$ up to a mass of 1.378 $M_\odot$ and eventually ignites carbon at the center with $\rho_c \sim 3 \times 10^9$ g cm^{-3} (NTY). Afterwards the white dwarf is assumed to undergo carbon deflagration until the transition to a late detonation takes place in the outer layers. The adopted carbon deflagration models are W7 and W8 (NTY), where the ratio between the mixing length and a scale height of pressure for convective deflagration is $l/H_p = 0.7$ (W7) and 0.8 (W8). Thus the propagation speed of the deflagration is faster in W8 (also C8) than W7 by a factor of ~ 1.2.

Since the difference in v_{def} between W7 and W8 (C8) is not large, both W7 and W8 may be marginal in inducing a late detonation. In the present study, therefore, we mainly study two cases of the late detonation in W7 with the transition from deflagration to detonation at $M_r = 1.12\ M_\odot$ (W7DT) and 1.20 $M_\odot$ (W7DN), respectively. These cases assume that a small difference in v_{def} in the inner layer leads to a significant difference in the transition point. In addition, the transition from the deflagration W8 to a late detonation at $M_r = 1.25\ M_\odot$ (W8DT) is simulated for comparison.

We also study the case with a rather artificial initial configuration where the white dwarf has a thick helium layer at $M_r > 1.20\ M_\odot$ (§ 4). The transition from W7 to late detonation is assumed to occur at the bottom of the helium layer (W7DHE).

The detonation wave is initiated by artificially accelerating v_{def} (Shigeyama et al. 1992). The initial composition in the unburned outer layers is set that the mass fractions of ^{12}C, ^{16}O, and ^{22}Ne are 0.48, 0.50, and 0.02 with a neutron excess of 0.002 ($Y_e = 0.499$). The hydrodynamical calculation is performed with a one-dimensional Lagrangian PPM code as in Shigeyama et al. (1992), and the detailed nucleosynthesis is calculated with a larger nuclear reaction network of 299 species (Thielemann, Nomoto, & Yokoi 1986; Thielemann, Hashimoto, & Nomoto 1990).

3. NUCLEOSYNTHESIS IN DEFLAGRATIONS AND LATE DETONATIONS

The early evolution of W7D's (W8DT) is the same as W7 (W8) (see NTY); a carbon deflagration wave forms at the center and propagates outward until the late detonation is initiated. Nucleosynthesis in the deflagration phase depends on the peak temperature T_p which decreases as the deflagration wave propagates outward because of the expansion of the white dwarf. In the interior to $M_r \lesssim 0.78\ M_\odot$ (0.90 $M_\odot$), the matter undergoes complete silicon burning to iron peak elements. In the very central region, neutronization due to electron capture leads to the production of ^{56}Fe, ^{54}Fe, and ^{58}Ni. At $0.78\ M_\odot \lesssim M_r \lesssim 1.02\ M_\odot$ ($0.90\ M_\odot \lesssim M_r \lesssim 1.05\ M_\odot$), incomplete silicon burning produces ^{56}Ni, Ca, Ar, S, and Si. At $1.02\ M_\odot \lesssim M_r \lesssim 1.28\ M_\odot$ ($1.05\ M_\odot \lesssim M_r \lesssim 1.35\ M_\odot$), explosive burning of oxygen and carbon produces Si to Ca.

At an assumed location, the deflagration wave is transformed into a detonation wave, which quickly develops to propagate self-consistently at the speed of a Chapman-Jouguet detonation. Behind the detonation wave, material undergoes explosive nuclear burning. Its products are sensitive to T_p, which in turn depends on the density at the burning front. For the same initial density, the detonation wave has a higher density than the deflagration because of the shock compression, thereby attaining a higher T_p. Accordingly, the detonation wave in the outer layers produces heavier elements than those produced by the deflagration in the inner layers. In other words, a composition inversion is naturally formed.

3.1. *Model W7DN*

In this case, the transition from deflagration to detonation is set to occur at $M_r = 1.20\ M_\odot$. At this stage, $T_p \sim 3 \times 10^9$ K behind the deflagration wave, and explosive carbon burning is forming O-Ne-Mg layers. The density ahead of the burning front is $\rho_0 = 1.7 \times 10^7$ g cm^{-3}. After the late detonation is started, T_p gets as high as 5×10^9 K. This temperature leads to incomplete silicon burning which synthesizes some ^{56}Ni and Si/Ca. At $1.21\ M_\odot < M_r < 1.28\ M_\odot$, the mass fraction of ^{56}Ni is $\sim$0.5–0.3, and the rest is Si, S, Ar, and Ca.

As the detonation wave propagates to the lower density layers, T_p decreases and explosive burning of oxygen, neon, and carbon takes place, accordingly. The resultant composition structure of W7DN is shown in Figure 1 as a function of the homologous expansion velocity v_{exp} and M_r. The production of ^{56}Ni by incomplete silicon burning extends from $v_{exp} \sim$ 14,000 to 30,000 km s^{-1}, and Ca, Ar, S, and Si are produced from explosive burning of oxygen, neon, and carbon up to $v_{exp} = 35{,}000$ km s^{-1} (Ca) and 50,000 km s^{-1} (Si). The mass of ^{56}Ni is $M_{Ni} = 0.63\ M_\odot$, and the explosion energy is $E = 1.4 \times 10^{51}$ ergs.

3.2. *Models W7DT and W8DT*

These models undergo the transition from deflagration to detonation at a higher density than W7DN, that is, $\rho_0 \sim 3.5 \times 10^7$ g cm^{-3} ahead of the deflagration wave. This corresponds to the transition at $M_r = 1.07\ M_\odot$ (W7DT) and 1.25 $M_\odot$ (W8DT) because of the difference in v_{def} between W7 and W8.

At the transition to the detonation, the peak temperature T_p increases from 4×10^9 to 5.5×10^9 K, which is significantly higher than in W7DN. Therefore, the material at

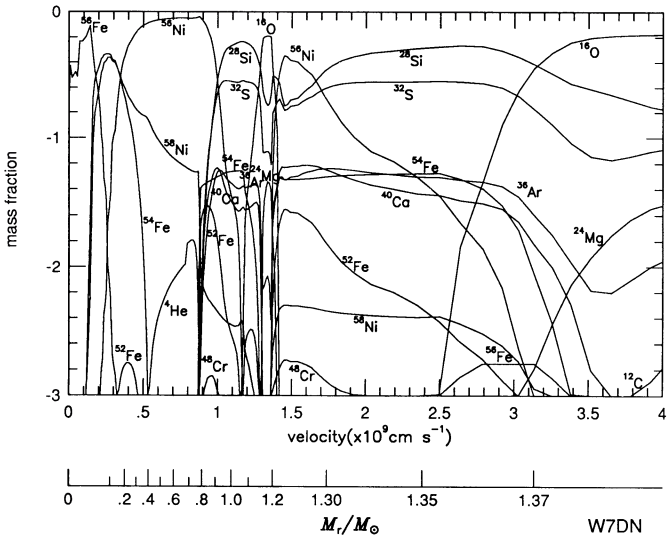

FIG. 1.—Composition of the late detonation model W7DN as a function of the expansion velocity and M_r, where the transition from deflagration to detonation takes place at $M_r = 1.20\ M_\odot$.

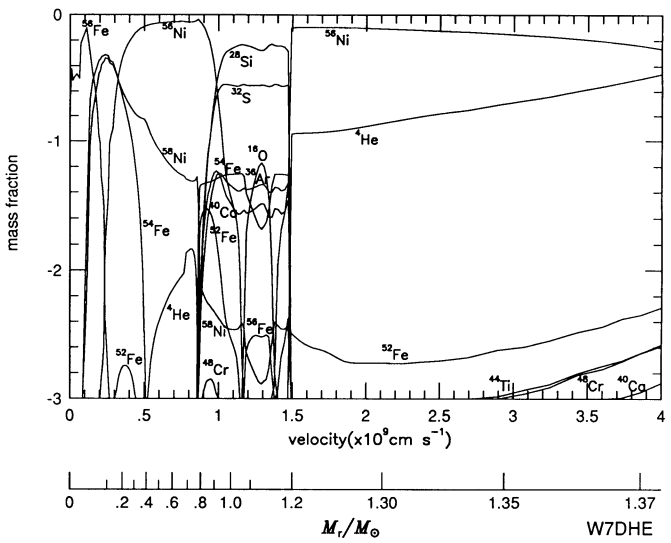

FIG. 3.—Same as Fig. 1 but for W7DHE with the transition at $M_r = 1.20\ M_\odot$. In the initial model, C+O at $M_r \geq 1.20\ M_\odot$ has been artificially replaced with helium.

1.07–1.17 $M_\odot$ in W7DT (1.25–1.32 $M_\odot$ in W8DT) undergoes almost complete silicon burning, producng mostly ^{56}Ni with a mass fraction as large as 0.9.

As the detonation wave propagates outwards, incomplete silicon burning takes place. The ^{56}Ni abundance decreases because of the lower T_p. The mass fractions of Ca and Si are still smaller than 0.03–0.05 at $M_r < 1.23\ M_\odot$ for W7DT ($M_r < 1.33\ M_\odot$ for W8DT), and the outer layers are rich in Si and Ca with small amounts of ^{56}Ni.

The composition structure of W7DT as a function of M_r and v_{exp} is shown in Figure 2. In velocity space, ^{56}Ni in the detonated layers extends from $\sim$12,000 to 30,000 km s^{-1} for W7DT (from 15,000 to 50,000 km s^{-1} for W8DT). Intermediate-mass elements are produced up to $v_{exp} \sim 40{,}000$ km s^{-1} (W7DT) and 50,000 km s^{-1} (W8DT) for Ca, and $\sim$50,000 km s^{-1} (W7DT) and 60,000 km s^{-1} (W8DT) for Si.

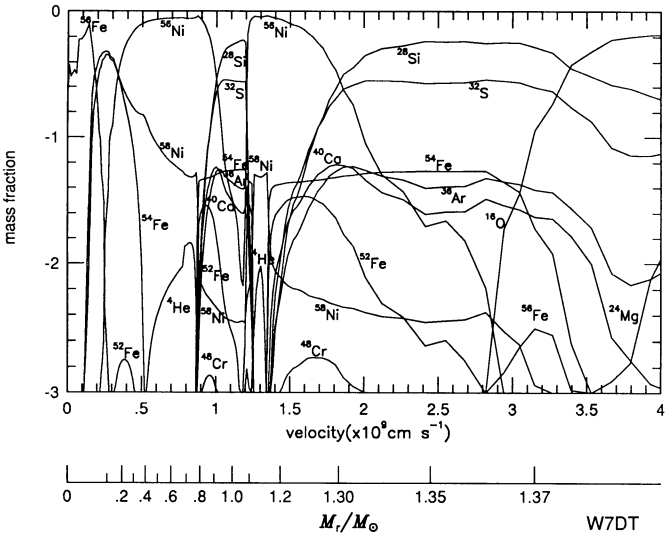

FIG. 2.—Same as Fig. 1 but for W7DT with the transition at $M_r = 1.13\ M_\odot$.

The explosion energy is 1.5×10^{51} ergs for both cases, and the ^{56}Ni masses are 0.78 $M_\odot$ (W7DT) and 0.80 $M_\odot$ (W8DT).

Figure 2 clearly reveals a composition inversion with an Fe-dominated layer above the Si-rich layer. Note that such an apparent composition inversion is not formed if the transition occurs where the deflagration is incinerating the material into iron peak elements as in the case of delayed detonation models (Khokhlov 1991b; Woosley & Weaver 1992).

3.3. *Model W7DHE*

This model undergoes the transition from deflagration to detonation at $M_r = 1.20\ M_\odot$ as in W7DN. Because of the presence of helium at $M_r > 1.2\ M_\odot$, the deflagration is naturally transformed into a helium detonation (i.e., without artificial acceleration of v_{def}).

Due to the larger energy release in a helium detonation than a carbon detonation, the peak temperature reaches $T_p \sim 6 \times 10^9$ K, being significantly higher than in W7DN. As seen in Figure 3, the detonated material is processed into a ^{56}Ni-dominated composition, where more than $\sim$10% helium by mass remains due to an α-rich freeze out. Almost no Si/Ca is produced except for the outermost layers at $M_r > 1.35\ M_\odot$ and $v_{exp} > 30{,}000$ km s^{-1}. The helium detonation also sends an inward shock wave, which burns O + Ne + Mg into Si-rich material. The produced explosion energy and the ^{56}Ni mass are larger than in other models as $E = 1.7 \times 10^{51}$ ergs and $M_{Ni} = 0.73\ M_\odot$.

4. COMPARISON WITH SN 1990N AND SN 1991T

The near and postmaximum spectra of SN 1991T and SN 1990N as well as other SNs Ia are well accounted for with the carbon deflagration model W7 (Harkness 1991; Jeffery et al. 1992). This implies that the composition structures in velocity space for the inner Si/Ca layers (layer 2) and the Fe-rich core (3) of W7DN, W7DT, and W7DHE are expected to be consistent with SN 1990N and 1991T. Then the question is whether the composition in the outermost layers (1) of these supernovae can be accounted for by these late detonation models.

Among the models presented in § 3, W7DN has a significant

amount of Si, Ca, and ^{56}Ni at expansion velocities as high as $v_{exp} \gtrsim 20{,}000$ km s^{-1}. The other three models (W7DT, W8DT, and W7DHE) have a Si/Ca layer being sandwiched by the Ni/Fe dominant layers. Therefore, the basic features of the Si and Fe distributions in W7DN and W7DT/W8DT/W7DHE are qualitatively in agreement with the spectroscopic features of SN 1990N and SN 1991T, respectively.

The three models W7DT/W8DT/W7DHE produce larger amounts of ^{56}Ni than W7DN, so that the resultant supernovae are brighter by ~ 0.2 mag. Their light curve shapes are basically similar to W7 (Shigeyama et al. 1992) except for slightly higher luminosities during the first ~ 10 days due to the outermost ^{56}Ni, which is in better agreement with observations.

For more detailed comparison with observations, we note that the outermost Ni-rich layer of W7DT and W8DT contains some high-velocity Si and Ca, while layer (1) of W7DHE contains a significant amount of He, and that these three models contain rather little O and Mg. Whether the amounts of Si/Ca, He, O/Mg are consistent with the premaximum spectra of SN 1991T should be examined with detailed synthetic spectra (Jeffery et al. 1992). Because of the presence of radioactive ^{56}Ni in the outermost layers, the spectra would be highly NLTE. Whether the helium features excited by γ-rays (Lucy 1991) appear or not would be a crucial diagnosis of not only W7DHE but also a possible alternative model of off-center helium detonations (Filippenko et al. 1992; Livne 1990; Nomoto 1982b).

With regard to O and Mg, it seems more likely that the transition to a detonation occurs at several points rather than in a spherical shell. The resulting carbon detonation may leave some unburned or partially burned C, O, Ne, and Mg.

The assumed thick helium layer in W7DHE might be realized if the accretion of helium takes place so slowly that helium is too cold to be ignited (Nomoto 1982a, b). Note, however, that such a slow accumulation of helium may occur only through nova explosions, thereby being extremely difficult, if not impossible. Also the central region of such a slowly accreting white dwarf must be solid, so that carbon burning at $\rho_c \sim 10^{10}$ g cm^{-3} is more likely to induce a collapse rather than an explosion (Nomoto 1987; Nomoto & Kondo 1991; Canal et al. 1990).

With these models, we suggest the following scenario for the variation among SNe Ia: There exist some variations in the ignition conditions, such as the central density and temperature of the white dwarf, due to variations of the white dwarf age and the mass accretion rate. This would result in a difference in v_{def}, which in turn leads to a somewhat larger difference in the density at the transition from deflagration to detonation. This results in a similar composition in the inner regions of layers 3 and 2, but a large variation of the composition in the outermost layer (1) such as in SN 1990N and SN 1991T. Cases like W7DN would be more common among SNs Ia, since the transition to detonation may occur more easily at lower densities because of smaller v_{CJ}/v_s and larger v_{def}/v_s. Some variations in the expansion velocities of Si may be due to the variation of the transition density.

We would like to thank David Jeffrey, Pilar Ruiz-Lapuente, Alex Filippenko, Bruno Leibundgut, and David Branch for stimulating discussions and valuable information. This work has been supported in part by the Ministry of Education, Science, and Culture in Japan (02302024 and 03218202) and NSF grant AST 8913799. Part of the calculations were performed at the NCSA (AST 890009N).

REFERENCES

Branch, D., Doggett, J. B., Nomoto, K., & Thielemann, F.-K. 1985, ApJ, 294, 619
Branch, D., & Tammann, G. A. 1992, ARA&A, in press
Branch, D., & Venkatakrishna, K. L. 1986, ApJ, 306, L21
Canal, R., Garcia, D., Isern, J., & Labay, J. 1990, ApJ, 356, L51
Filippenko, A. V., et al. 1992, ApJ, 384, L15
Harkness, R. P. 1991, in SN 1987A and Other Supernovae, ed. I. J. Danziger & K. Kjäer (Garching: ESO), 447
Jeffery, D. J., Leibundgut, B., Kirshner, R. P., Benetti, S., Branch, D., & Sonneborn, G. 1992, ApJ, in press
Kohkhlov, A. M. 1991a, A&A, 245, 114
———. 1991b, A&A, 245, L25
Leibundgut, B., Kirshner, R. P., Filippenko, A. V., Shields, J. C., Foltz, C. B., Phillips, M. M., & Sonneborn, G. 1991, ApJ, 371, L23
Livne, E. 1990, ApJ, 354, L53
Lucy, L. B. 1991, ApJ, 383, 308
Nomoto, K. 1982a, ApJ, 253, 798
———. 1982b, ApJ, 257, 780
———. 1987, in IAU Symp. 125, The Origin and Evolution of Neutron Stars, ed. D. J. Helfand & J.-H. Huang (Dordrecht: Reidel), 281
Nomoto, K., & Kondo, Y. 1991, ApJ, 367, L19
Nomoto, K., Thielemann, F.-K., & Yokoi, K. 1984, ApJ, 286, 644 (NTY)
Nomoto, K., Yamaoka, H., Shigeyama, T., Kumagai, S., & Tsujimoto, T. 1992, in Supernovae (Les Houches, Session LIV), ed. J. Audouze et al. (Amsterdam: Elsevier), in press
Phillips, M. M., Wells, L. A., Suntzeff, N. B., Hamuy, M., Leibundgut, B., Kirshner, R. P., & Foltz, C. B. 1992, AJ, in press
Ruiz-Lapuente, P., Cappellaro, E., Turatto, M., Gouiffes, C., Danziger, I. J., Della Valle, M., & Lucy, L. B. 1992, ApJ, 387, L33
Shigeyama, T., Nomoto, K., Yamaoka, H., & Thielemann, F.-K. 1992, ApJ, 386, L13
Thielemann, F.-K., Hashimoto, M., & Nomoto, K. 1990, ApJ, 349, 222
Thielemann, F.-K., Nomoto, K., & Yokoi, K. 1986, A&A, 158, 17
Williams, F. A. 1985, Combustion Theory (Menlo Park: Benjamin/Cummings), 217
Woosley, S. E., & Weaver, T. A. 1986, Lecture Notes in Physics, 255, 91
———. 1992, in Supernovae (Les Houches, Session LIV), ed. J. Audouze et al. (Amsterdam: Elsevier), in press